JOURNAL OF AIRCRAFT
Vol. 47, No. 2, March–April 2010

Aircraft Vortex Wake and Flight Safety Problems

Anatoliy V. Bobylev*
Central Aero-Hydrodynamics Institute, 140180, Moscow, Russia
Victor V. Vyshinsky†
Moscow Institute of Physics and Technology, 140181, Moscow, Russia
and
George G. Soudakov‡ and Vassiliy A. Yaroshevsky§
Central Aero-Hydrodynamics Institute, 140180, Moscow, Russia

DOI: 10.2514/1.46432

The paper presents a mathematical model of the aircraft vortex wake for evaluating the safe separation considering the wake-generating and following aircraft types and weather conditions. The solution of four major problems is contained in the model concerned, namely, the wake generator, the interaction of the following aircraft with the preceding aircraft vortex, the description of the turbulent atmosphere, and the vortex destruction. Verification of the model was made based on experimental results of wind-tunnel and flight tests. Given are calculations of the wake characteristics aft of particular aircraft and safe distance values in landing with various turbulent atmosphere states.

Nomenclature

b	=	distance between vortices, m, where b_0 is the initial distance
$b_{ik}(\Omega)$	=	correlation tensor in Ω space
$E(\Omega)$	=	energetic function of spectral density
H	=	flight altitude, m
k	=	turbulent energy, m^2/s^2
L	=	wingspan, m
L_t	=	turbulence scale, m
L_u, L_v, L_w	=	scales of turbulent gust components, m
Pr_T	=	Prandtl number based on temperature
Pr_w	=	Prandtl number based on velocity
q_t	=	turbulence level, m/s, $\sqrt{3}\sigma_w$ for isotropic turbulence
Ri_T	=	Richardson number based on temperature
Ri_w	=	Richardson number based on velocity
r	=	distance from the vortex axis, m
r_c	=	vortex core radius, m
$S = \sqrt{2S_{ij}S_{ij}}$, $S_{ij} = \frac{1}{2}\left(\frac{\partial V_i}{\partial x_j} + \frac{\partial V_j}{\partial x_i}\right)$	=	Navier–Stokes symmetric tensor
$S_j(\Omega)$	=	spectral density of j component of the gust
T	=	temperature, K
t	=	time, s
U_∞	=	flight velocity, m/s
u, v, w	=	longitudinal, lateral, and vertical velocity components, m/s
V	=	wind velocity, m/s
V_τ	=	circumferential velocity in the vortex, m/s
x, y, z	=	longitudinal (along the vortex axis), horizontal, and vertical coordinates, m
α	=	angle of attack
Γ	=	vortex circulation, m^2/s, where Γ_0 is the circulation at the initial moment of time
Γ_c	=	vortex core circulation, m^2/s
$\Delta y, \Delta z$	=	deviations of axial line from undisturbed position, m
$\Delta\hat{y}, \Delta\hat{z}$	=	Fourier transformation for deviations
ε_t	=	turbulent energy dissipation rate, m^2/s^3
μ	=	molecular air viscosity coefficient, $kg/s^2{\cdot}m^2$
ρ	=	air density, kg/m^3
$\sigma_u, \sigma_v, \sigma_w$	=	mean-square deviations of turbulent gust components, m/s
τ	=	nondimensional time, $\frac{t\Gamma}{2\pi b_0^2}$
ν	=	molecular kinematic viscosity, m/s^2
ν_e	=	effective kinematic viscosity, m/s^2, $\nu_t + \nu$
ν_t	=	turbulent viscosity, m/s^2
ω	=	vorticity, s^{-1}
Ω	=	vector of spatial frequency, $(\Omega_x, \Omega_y, \Omega_z)$

I. Introduction

WHEN in flight in the atmosphere, an aircraft generates a vortex wake that is dangerous for other flying vehicles. In takeoff and landing modes, it is the vortex wake limitation that specifies the safe distance between the aircraft. A decrease in the distance, with the safety target being maintained, increases the airport handling capacity.

There exists at present an International Civil Aviation Organization (ICAO) matrix that accumulates the entire aviation experience and ensures safe aircraft takeoff and landing. The matrix concerned specifies the aircraft safe separation considering the types of the preceding and following aircraft. Yet the air traffic controller, guided by his personal experience, often decreases the allowable safe distance value. According to the summary review [1], flight accidents due to the aircraft getting into a vortex wake frequently occurred during landing by the flight controller instructions. A similar problem arises in a cruise flight. The problem becomes still more pressing as the possibility of decreasing the flight level separation is now under consideration. It is, therefore, extremely important to have a reliable mathematical model to evaluate aircraft safe separation considering their types and weather conditions (an extended safe separation matrix). A mathematical model like that should be based

Received 22 July 2009; revision received 27 December 2009; accepted for publication 5 January 2010.

*Head of Subdivision, Department of Flight Dynamics, 1, Zhoukovsky Street, Zhoukovsky.
†Dean, Department of Aeromechanics and Flight Engineering, 16, Gagarin Street, Zhoukovsky. Senior Member AIAA.
‡Head of Division, Department of Aerodynamics, 1, Zhoukovsky Street, Zhoukovsky.
§Chief Scientist, Department of Flight Dynamics, 1, Zhoukovsky Street, Zhoukovsky.

on the solution of the four major problems, namely, the wake-generator flight, the interaction of the follower with the vortex wake from the preceding aircraft, the description of the turbulent atmosphere, and the vortex destruction.

It should be noted that no wake mathematical model known so far is complete, that is, able to solve all the four problems as a single complex. Out of the models available at present, the following are worth mentioning.

The NASA model [2] simulates the turbulent atmosphere surface layer and vortex wake evolution using a large eddy simulation method known as 3-D LES. With this, both stages of the vortex wake destruction are described. The wake-generator flight is studied with the aid of an engineering model that specifies far vortex wake evolution initial conditions. However, following aircraft and respective safe separation criterion were not addressed by the NASA model. The model also contains an atmosphere surface layer description close to that given in the present review.

The European investigations were devoted to the perfection of the methods for simulating the vortex wake destruction based on 3-D LES. The problem of an aircraft getting into a wake was also studied extensively. A cycle of experimental studies has been carried out. A summary of the investigations conducted in this field is given in [1].

The model used by Belotserkovsky et al. [3] applied a discrete vortex method for solving both the first and second aircraft problems and the vortex wake evolution. The atmosphere surface layer model is represented by a single parameter: the Richardson number that specifies the vortex turbulent diffusion rate. The constant altitude wind velocity profile is used.

The Central Aerohydrodynamics Institute model [4–6] and the packages of programs developed on its basis contain solutions for all four problems. The wake-generator problem is solved within the framework of the boundary-value problem for the three-dimensional Reynolds-averaged Navier–Stokes equations (3-D RANS) or by the panel method. The problem of the follower is solved by the panel method. The turbulent atmosphere mathematical model is based on the Kolmogorov (cruise flight) and Monin–Obukhov (atmosphere surface layer) theories as well as on the Experimental Meteorology Institute studies. Both the near and far wakes are simulated using the two-dimensional Reynolds equations (2-D RANS) and an ad hoc constructed algebraic turbulence model.

Along with the models considered, simplified mathematical wake models that are described by simple analytical formulas are also available. For example, the distribution of the velocity tangential component V_τ generated by one vortex may have the following form:

$$V_\tau = \frac{\Gamma}{2\pi r}\frac{r^2}{(r^2 + r_c^2)} \tag{1}$$

where Γ is the vortex circulation, r is the vortex axis distance, and r_c is the vortex core radius corresponding to the velocity maximum. Part of the investigation of the dynamics of flight was performed using a simplified mathematical wake model Eq. (1).

An essential result of the present investigation was the construction of a unified model of wake destruction in the turbulent atmosphere that combined the turbulent atmosphere and wake destruction models and enabled the effect of weather conditions on the wake life span to be taken into account. A set of results important for practical application has been obtained: an extended safe separation matrix for a landing approach was suggested and a conclusion was drawn that the A380 aircraft does not fit in with the ICAO regulations; therefore, a new super heavy aircraft type must be introduced [4]. This conclusion was confirmed by the Airbus Industries flight tests.[¶]

II. Mathematical Model of Vortex Wake in Turbulent Atmosphere

The model proposed is composed of the wake-generator units, near vortex wake, turbulent atmosphere, far vortex wake, and vortex interaction with the follower. A block diagram of the program package is presented in Fig. 1, where V is the wind velocity, T is the temperature, k is the turbulent energy, and L_t is the turbulence scale.

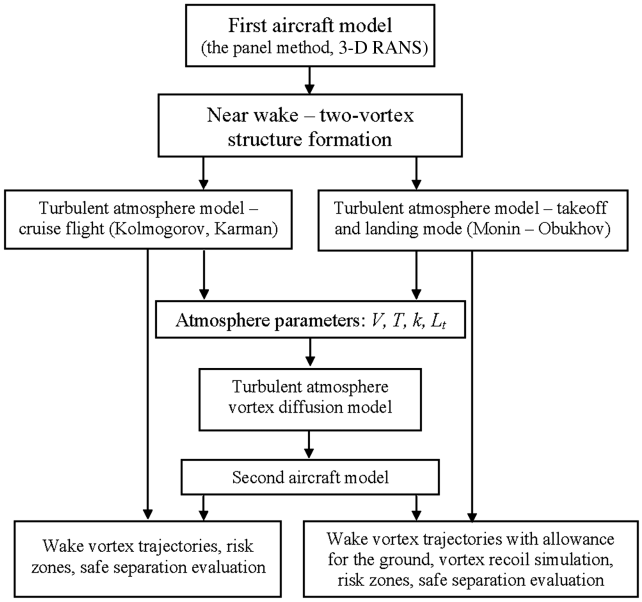

Fig. 1 Block diagram of the program package.

To calculate the flow about the wake generator along with the boundary element methods [7], a package of programs for solving the boundary-value problem for 3-D RANS with a k–ω shear strain transport (SST) turbulence model is used that enables the near-field characteristics and wake initial conditions to be defined without any additional assumptions. Figure 2 presents an example of this calculation for a Tu-204 aircraft at an angle of attack of $\alpha = 3$ deg, a Mach number of $M = 0.78$, and a Reynolds number of $Re = 2 \times 10^6$.

The near wake zone is defined as the area aft of the aircraft for which the input boundary is located at a distance of $x_{\text{in}} \sim 0.5L$ and the output one is located at a distance of $x_{\text{out}} \sim (6\text{–}10)L$, where L is the wingspan. The output boundary is specified by the condition of the vortex sheet folding in a coherent vortex system (in two vortices, as a rule). The ultimate result of the near wake simulation is the output boundary parameters of the flow distribution.

To calculate the near wake aft of the aircraft, the following are used: an unsteady analogy in the approximation of the 2-D unsteady Reynolds-averaged Navier–Stokes equations (URANS) with an ad hoc constructed algebraic turbulent viscosity model or a modified k–ε turbulence model, 3-D RANS, or analytical models.

As the initial condition for the near wake simulation, the calculation result is used with $x = x_{\text{in}}$ for the complete aircraft layout. Analytical models relate the input boundary vortex parameters immediately to the aircraft performance.

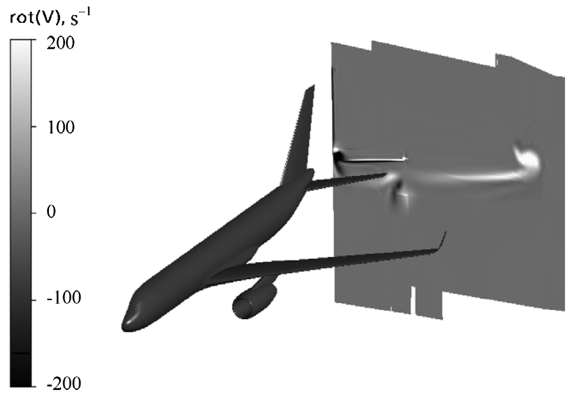

Fig. 2 Aircraft layout and longitudinal component of vorticity field in the cross section $x = 0.5L$.

[¶]Press release of Airbus Industries, 28 September 2006; press release of Airbus Industries, 3 October 2006; press release of the European Aeronautic Defence and Space Company, 3 October 2006.

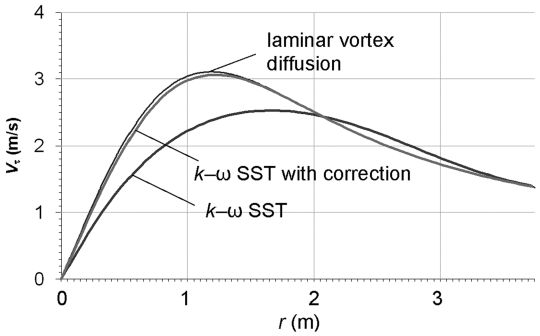

Fig. 3 Tangential velocity component vs vortex center distance.

In the unsteady analogy approximation, instead of a three-dimensional stationary wake evolution problem an equivalent two-dimensional nonstationary one is solved ($t = x/U_\infty$, where U_∞ is the flight velocity). The problem concerned involves formulation of the initial conditions at $t = 0$. The initial conditions are taken from the calculation of a flow about a complete aircraft layout using 3-D RANS for the cross section $x = x_{\text{in}}$.

To examine the adequacy of a standard k–ω SST turbulence model, an individual vortex problem was used as an example. The experiments show that in the vortex core there occurs laminarization of the flow and the turbulent viscosity tends to zero. The standard turbulence model is seen (Fig. 3) to give an inadequate result due to the excessive turbulent viscosity in the zones of severe flow vorticity. Hence, a modified k–ω SST turbulence model with a correction for the streamline curvature should be used [8] (Fig. 3).

The three-dimensional stationary near vortex wake problem (3-D RANS) is solved in the rectangular area. At the input boundary ($x_{\text{in}}/L = 0.5$), three velocity components and the pressure taken from the solution of the problem of a flow about the aircraft's complete layout are specified. At the output boundary ($x_{\text{out}}/L =$ 7.73) set are zero derivatives in x coordinate of the problem parameters and at the lateral boundaries the static pressure is specified. The problem is solved for half the space with an assumption of the flow symmetry relative to the longitudinal vertical plane $z = 0$.

Figure 4 gives calculation results of the field of the longitudinal vorticity component ω_x in the cross section $x_{\text{out}} = 7.73L$ obtained using 2-D URANS and 3-D RANS. For the 3-D RANS case, the flow velocity longitudinal component is also presented (Fig. 5). The main difference between the 3-D RANS and 2-D URANS methods is that the former allows for the flow velocity longitudinal component and its effect on the lateral components. The effect is seen to be negligible, which confirms the correctness of the unsteady analogy application.

Figure 5 also shows the trailing vortex core longitudinal velocity deficit of about 20 m/s at a flow velocity of 225 m/s. The vortex characteristics in the output section $x_{\text{out}} = 7.73L$ are presented in Table 1.

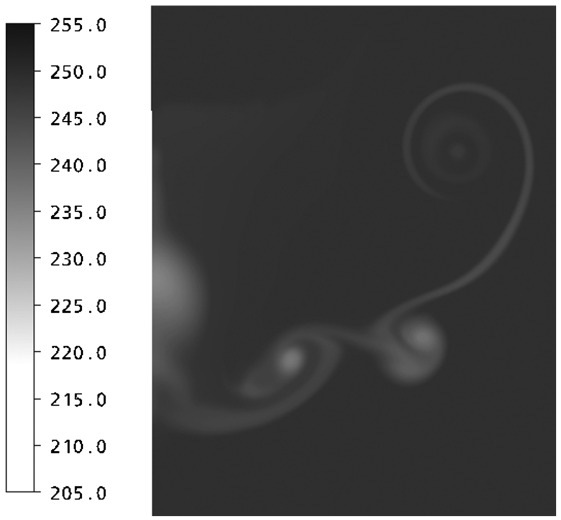

Fig. 5 Field of the longitudinal velocity component (in meters per second).

III. Calculation of Aircraft Aerodynamic Characteristics When Entering a Vortex Wake

To obtain the integral characteristics (forces and moments) exerted on an aircraft when entering a vortex wake from the preceding aircraft, the panel methods and the discrete vortex method are used. To estimate an admissible rolling moment, calculations were made for a number of wake generators and various vortex wakes. The vortex field induced by the wake generator was described by the analytical model. Estimations have been made based on the maximum admissible rolling moment induced by the vortex from the preceding aircraft on the following aircraft moving along the vortex axis.

The vortex circulation value that is hazardous for the follower appeared to be negligibly dependent on the vortex core radius. Figure 6 gives a generalized dependence of the wake-generator vortex circulation admissible for the follower versus its wing span L.

This dependence was obtained by means of estimation of the maximum admitted roll moment induced by the vortex with given circulation on the following aircraft flying along the vortex axis (the worst case). To estimate this admitted roll moment, calculations for complete layouts immersed in the vortex wake were carried out using a panel method [7]. The vortex structure depending on the wake-generating aircraft parameters was described by the formula (1). It was obtained that additional rolling moment induced by the vortex weakly depends on the vortex core radius; therefore, this parameter is absent in Fig. 6. Because only the increment of rolling moment induced by the vortex is important, the aircraft height above the ground is also absent in Fig. 6.

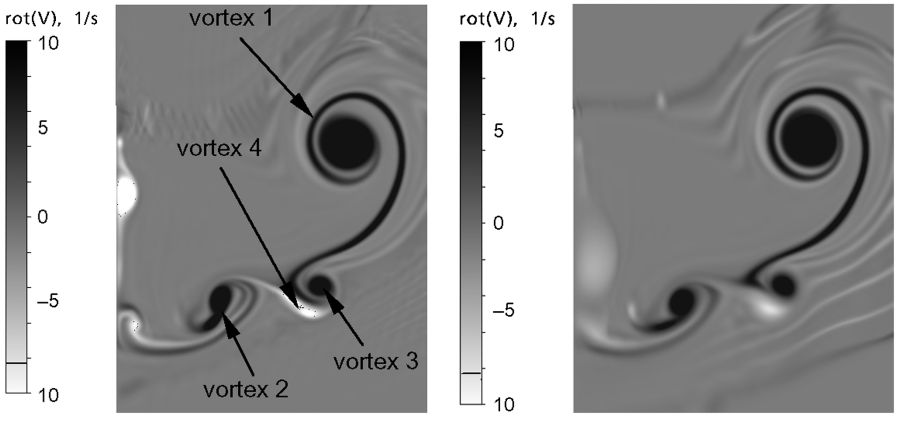

Fig. 4 Field of the longitudinal vorticity component ω_x: a) 2-D URANS, and b) 3-D RANS.

Table 1 Core radius r_c and vortex circulation Γ

	Unsteady analogy 2-D URANS				3-D RANS			
	Vortex 1	Vortex 2	Vortex 3	Vortex 4	Vortex 1	Vortex 2	Vortex 3	Vortex 4
r_c, m	0.91	0.77	0.77	0.59	0.99	0.87	0.82	0.91
Γ, m^2/s	370	61	36	−7	356	65	25	−10

Given this relationship and the wake destruction mathematical model (i.e., wake-generator vortex circulation as a function of time), the time interval required to provide the following aircraft safe flight may be estimated.

IV. Far Wake Evolution and Destruction

In simulating the vortex wake destruction in the turbulent atmosphere in a cruise flight, the model of an isotropic uniform atmosphere is used. The initial data for setting random velocities of the turbulent wind gusts are a spectral density form and two parameters: scale and variance. The most common is the Karman spectral density model [9]:

$$E(\Omega) = \frac{55}{9\pi}\sigma^2 L_t \frac{(\alpha_k L_t \Omega)^4}{[1 + (\alpha_k L_t \Omega)^2]^{17/6}} \tag{2}$$

where L_t is the turbulence scale, σ is the standard deviation, $\alpha_k = 1.339$ is the Karman constant, and $\Omega = |\boldsymbol{\Omega}|$ is the spatial frequency vector magnitude $\boldsymbol{\Omega} = (\Omega_x, \Omega_y, \Omega_z)$. Function $E(\Omega)$ enables spectral densities of the gust velocity random vector components of any order to be determined. Thus, the correlation tensor $b_{ik}(\Omega)$ that specifies variance and correlation of the velocity components in the Ω space is determined by the following formula [10]:

$$b_{ik}(\Omega) = \frac{E(\Omega)}{4\pi} \cdot \frac{(\Omega^2 \delta_{ik} - \Omega_i \Omega_k)}{\Omega^4}$$

Hence, the jth component spectral density has the form [9]

$$S_j(\Omega_x, \Omega_y, \Omega_z) = b_{jj} = \frac{E(\Omega)(\Omega^2 - \Omega_j^2)}{4\pi\Omega^4}$$

(without summation on the repetitive index j). It should be emphasized that in the Ω space there is no frequency correlation (as a result of the turbulence uniformity and isotropy).

Spectral densities of a fewer number of variables are determined by means of integration:

$$S_j(\Omega_x, \Omega_y) = \int_{-\infty}^{\infty} S_j(\Omega_x, \Omega_y, \Omega_z)\, \mathrm{d}\Omega_z,$$

$$S_j(\Omega_x) = \int_{-\infty}^{\infty} S_j(\Omega_x, \Omega_z)\, \mathrm{d}\Omega_z$$

These formulas are valid for the isotropic turbulence when spectral characteristics are identical for all the directions. In practice, this hypothesis is applied to altitudes above 300 m, at which variances and turbulence scales of all the velocity vector components are taken to be identical:

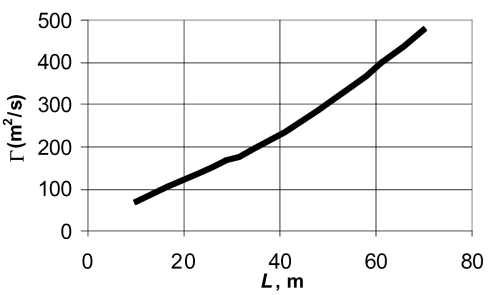

Fig. 6 Maximum admissible wake-generator circulation Γ for the aircraft with wingspan L moving along the vortex axis to safely get into the preceding aircraft wake.

$$L_u = L_v = L_w = \begin{cases} h & \text{for } h < 760 \text{ m}, \\ 760 \text{ m} & \text{for } h > 760 \text{ m} \end{cases} \qquad \sigma_u = \sigma_v = \sigma_w$$

In the atmosphere surface layer ($h < 300$ m), spectral density parameters of various wind velocity components are different and vary with height. There exists a great number of models that are applicable to the aircraft landing simulation, for instance, the Boeing model [11]:

$$\frac{\sigma_u}{\sigma_w} = \frac{\sigma_v}{\sigma_w} = \frac{1}{[0.177 + 0.823\frac{h}{300}]^{0.4}}, \qquad L_w = h$$

$$L_u = L_v = L_w \left(\frac{\sigma_u}{\sigma_w}\right)^3$$

or the ICAO model [12]:

$$L_w = h, \qquad L_u = L_v = 180 \text{ m}, \qquad \sigma_u = \sigma_v = 2\sigma_w$$

Here $\sigma_w \approx 0.09 U_{10}$, where U_{10} is the systematic wind modulus at the height of 10 m. In practice, spectral density formulas used for the atmosphere surface layer are the same as those for the isotropic turbulence, but in dimensionless variables:

$$\bar{S} = \frac{S}{\sigma^2}, \qquad \bar{\Omega}_i = \frac{\Omega_i}{L_i^j}, \qquad \bar{x} = \frac{x}{L_x^j}, \qquad \bar{y} = \frac{y}{L_y^j}, \qquad \bar{z} = \frac{z}{L_z^j}$$

where L_i^j is the scale of the jth velocity component along the ith axis. One-dimensional (in x) and two-dimensional (in x and z) dimensionless spectral densities of the turbulence are determined by the following formulas:

$$\bar{S}_v(\bar{\Omega}_x) = \bar{S}_w(\bar{\Omega}_x) = \frac{1 + \frac{8}{3}(\alpha_k \bar{\Omega}_x)^2}{\pi[1 + (\alpha_k \bar{\Omega}_x)^2]^{11/6}}$$

$$\bar{S}_v(\bar{\Omega}_x, \bar{\Omega}_z) = \frac{2\alpha_k^2[1 + \frac{11}{3}(\alpha_k \bar{\Omega}_x)^2 + (\alpha_k \bar{\Omega}_z)^2]}{3\pi[1 + (\alpha_k \bar{\Omega}_x)^2 + (\alpha_k \bar{\Omega}_z)^2]^{7/3}}$$

$$\bar{S}_w(\bar{\Omega}_x, \bar{\Omega}_z) = \frac{16\alpha_k^2[(\alpha_k \bar{\Omega}_x)^2 + (\alpha_k \bar{\Omega}_z)^2]}{9\pi[1 + (\alpha_k \bar{\Omega}_x)^2 + (\alpha_k \bar{\Omega}_z)^2]^{7/3}}$$

Dimensional and dimensionless spectral densities are related by ratios $S_j(\Omega_x) = \sigma_j^2 \bar{S}_j(\bar{\Omega}_x) L_x$, $S_j(\Omega_x, \Omega_z) = \sigma_j^2 \bar{S}_j(\Omega_x, \Omega_z) L_x L_z$. The spectral densities presented are normalized so that the respective variances are determined by integrating only over the positive frequencies.

Known spectral densities for various components enable random realizations of gust velocities to be specified. The most common way of specifying the realizations is to represent wind velocities in the form of the Fourier series with discrete frequency set:

$$W_j(x, y, z) = \sum_{m=1}^{M} \sum_{k=1}^{K} \sum_{n=1}^{N} A_{mkn}^j \cos(\Omega_{xm} x + \Omega_{yk} y + \Omega_{zn} z) + B_{mkn}^j \sin(\Omega_{xm} x + \Omega_{yk} y + \Omega_{zn} z) \tag{3}$$

where A_{mkn}^j and B_{mkn}^j are independent (in terms of indices m, k, and n) Gaussian random variables with variances $D[A_{mkn}^j] = D[B_{mkn}^j] = S_j(\Omega_{xm}, \Omega_{yk}, \Omega_{zn}) \Delta\Omega_x \Delta\Omega_y \Delta\Omega_z$, but dependent in terms of index j. The correlation factor is specified by tensor b_{ik}.

Random realizations are presented in the form of the Fourier series with prescribed discrete frequency set $\Omega_k = k\Delta\Omega$, $k = 1, 2, \ldots, K$. The frequencies are determined by discretization of the OX axis and

selected so that the discrete spectrum includes all the frequencies for which the respective harmonics may practically be realized with the given discretization of the independent variable x. The minimum frequency in the expansion is determined so that its respective wavelength coincides with the entire realization length and the maximum one is determined by the wavelength corresponding to about four steps of the OX axis discretization. In this case,

$$\Omega_1 = \Delta\Omega = 2\pi/(x_M - x_1), \qquad K = M/4$$

The random realization calculation procedure is based on the lack of different harmonic correlation and reduced to the following. For each frequency determined is the mutual spectral density symmetric matrix S^k with elements $S^k_{i,j} = S_w(b_{yij}, b_{zij}, \omega_k)\Delta\omega$ where $i = 1, 2, \ldots, N$, $j = 1, 2, \ldots, N$, $b_{yij} = y_i - y_j$, and $b_{zij} = z_i - z_j$. The symmetric matrix S^k is presented in the following form:

$$S^k = T^k(T^k)^T$$

where matrix T is proportional to the orthogonal transformation matrix that reduces the symmetric matrix to a diagonal-type. When calculated numerically, matrix T is determined by an iterative method of rotations that allows any symmetric matrix to be reduced to a diagonal-type irrespective of the multiplicity of its eigenvalues. With matrix T having been determined, the respective harmonics of all the random realizations can be obtained as linear combinations of noncorrelated standard harmonics having the same frequency:

$$w^k_{n,m} = \sum_{j=1}^{N} T^k_{nj}\xi^k_j(x_m) \tag{4}$$

where $\xi^k_j(x_m) = B^k_j \cos(\Omega_k x_m) + C^k_j \sin(\Omega_k x_m)$, and B^k_j and C^k_j are independent standard normally distributed random quantities (with a zero average of distribution and unit variance). Equation (4) is used to calculate all the values of indices n and m, that is, at specified frequency Ω_k, the respective harmonics of all the wind realizations over their entire length are determined. The ultimate result is obtained by the summation of all the harmonics:

$$w_{nm} = \sum_{k=1}^{K} w^k_{nm}$$

A. Atmosphere Surface Layer

The atmosphere surface layer is characterized by the altitude profiles of the average wind velocity, temperature, and turbulence level and scale (or turbulent energy dissipation rate). It should be emphasized that all four functions are essential for the wake evolution description, but they are not independent. The object of the mathematical model of the atmosphere surface layer is to find a correlation between the profiles of the average wind velocities and temperature and those of turbulence level and scale. The simplest and most efficient method at present is a mathematical model of the atmosphere based on the Monin–Obukhov theory, which contains two parameters (wind velocity at a particular altitude and the Obukhov length or related to the latter Richardson number describing the atmosphere stability). Based on these parameter values, the model allows all four necessary functions to be reconstructed using the similarity theory considerations and empirical relationships. Vyshinsky et al. [4] gave a detailed description of the model in which, as an illustration, the wind velocity profiles for different atmosphere states as well as a comparison of the computational results with the experimental data was presented.

B. Model of Vortex Wake Destruction in Turbulent Atmosphere [5,6]

This model is based on the solution of the boundary-value problem for 2-D URANS. As shown earlier, the turbulence model correction for the streamline curvature is required. Yet, in the far field this correction is not sufficient due to the interaction between the background turbulence and that generated by the wake vortices. The present paper suggests two turbulence models, an algebraic one and a k–ω SST, that evidently take into account the aforementioned interaction. The correction involved should make an allowance for the two essentially different scales present in the problem. As the size of the calculational domain is usually less than the atmosphere turbulence scale, the effect of the turbulent energy transfer from the large atmosphere turbulent vortices to the scales of the aircraft-generated vortex should be taken into account.

C. Turbulence Models

The algebraic two-scale turbulence model serves to generalize the results [5,6]. The vortex ambient atmosphere is described by the two parameters: turbulence level $q_t = (\overline{u'^2} + \overline{v'^2} + \overline{w'^2})^{1/2}$ and turbulence scale L_t. The turbulence scale inside the vortex is much less than that of the atmosphere $\ell \ll L_t$. Based on the dimension theory, the turbulent energy dissipation rate ε_t may be expressed through the quantities involved as follows:

$$\varepsilon_t = C_0(q_t^3/L_t)$$

where C_0 is some constant. By means of a cascade process, the atmosphere turbulent energy should be transferred to the smaller scales (including those on the order of the wake vortex size) before it dissipates into heat. As the size of the real wake problem computational domain does not allow the evolution of large vortices with sizes on the order of L_t to be simulated (they may be simulated only in 3-D statement), the energy influx from the large atmosphere turbulent vortices should explicitly be taken into account in the turbulent energy balance equation. The total influx of the vortex turbulent energy is equal to the sum of the energy production in the vortex and energy influx from the large atmosphere vortices:

$$P = \rho\left[\nu_t\left(1 - \frac{Ri_T}{Pr_T} + \frac{Ri_w}{Pr_w}\right)S^2 + C_0\frac{q_t^3}{L_t}\right]$$

where $S = \sqrt{2S_{ij}S_{ij}}$, $S_{ij} = \frac{1}{2}\left(\frac{\partial V_i}{\partial x_j} + \frac{\partial V_j}{\partial x_i}\right)$ is the Navier–Stokes tensor, $\nu_t = \mu_t/\rho$ is the turbulent kinematic viscosity coefficient, and μ_t is the turbulent viscosity coefficient of air. The terms containing Richardson numbers are responsible for the energy production by the temperature gradient and that of the longitudinal velocity, respectively. Then the hypothesis of the local turbulent energy balance may be expressed as follows:

$$C_v^2\frac{\nu_t(1 - Ri_T/Pr_T + Ri_w/Pr_w)}{Re}S^2 + C_q^3\frac{q_t^3}{L_t} = \frac{\nu_t^3}{\ell^4}$$

where C_v and C_q are some constants. Following [13], in the equation above, a correction for the Reynolds number is introduced into the term responsible for the turbulent energy production, where $Re = \Gamma_c/\nu$, Γ_c is the vortex core circulation, $\nu = \mu/\rho$ is the molecular kinematic viscosity coefficient, and μ is the molecular air viscosity coefficient. The correction enables the above equation to be applied in cases of both full-scale and wind-tunnel conditions. The term on the right-hand side of the equation describes the turbulent energy dissipation on the scale at which viscosity is essential. In the presence of the turbulent background, the turbulent energy dissipation is greater than in the absence of the external turbulence. There results a cubic equation for determining the turbulent viscosity. As for the constants, values $C_v = 0.05$ and $C_q = 0.03$ were obtained.

From the physical point of view, it is evident that turbulence scale ℓ is not constant. It increases from zero in the vortex center up to the value on the order of the vortex size (or the distance between vortices b) at some distance away from the vortex. In [14], asymptotic estimates for ℓ were obtained in the vortex center and outside the vortex core. Also, a composite formula for ℓ in the entire vortex

region was suggested there. The formula is used in the present paper and may be expressed as follows:

$$\ell^2 = \ell_0^2 \frac{S}{\sqrt{C_\omega \omega^2 + S^2}}$$

It should be noted that the relationship involved is a means of allowing for the streamline curvature in the algebraic turbulence model. Based on the results of the testing, the following values of ℓ_0 (typical vortex size) and C_ω were taken on:

$$C_\omega = 1.5, \qquad \ell_0 = \sqrt{S_0/\pi}$$

where S_0 is the area occupied by the vortex (where 99% of the whole circulation is concentrated).

Along with the algebraic turbulence model, a modified k–ω SST model is used. As indicated earlier, a standard version of this model is inapplicable to the problem considered due to an extremely high vortex core turbulent viscosity value and the presence of the two turbulence scales (an atmosphere background turbulence and a vortex-induced one) that are essentially different in value. Both the equations are subject to modification. A turbulent energy generation corrector for streamline curvature suggested by Shur et al. [8] was used and a term describing the influx of the turbulent energy from the atmosphere background turbulence into the vortex region was introduced. The last one is completely analogous to the respective term in the algebraic turbulence model.

D. Two-Phase Semi-Empirical Turbulence Model

According to [1], the vortex destruction process has two phases: that of slow diffusion (vortex diffusion at low velocity) and subsequent fast destruction. The two phases are separated by characteristic time T^*. In compliance with the experimental results and calculations, based on the large eddy simulation (see [1]), one obtains:

$$T^* = (2 \cdots 6)t_0; \qquad t_0 = (2\pi b^2/\Gamma_0)$$

A physical process of circulation loss in the turbulent diffusion phase may be represented as follows:

1) Vortex turbulent diffusion is induced both by the vortex itself (velocity gradients) and the external atmosphere.

2) The effect of the external atmosphere on the turbulent viscosity prevails at high r.

3) In compliance with the model used in [2], an appreciable fraction of the vortex vorticity exists at sufficiently high r.

4) The present paper assumes the following hypothesis: the vortex vorticity below that of the background atmosphere is not registered by any physical device and cannot be identified as the vorticity belonging to the vortex.

5) In the process of turbulent diffusion, increasingly larger vortex regions have vorticity values lower than the background one. This results in the vortex circulation loss.

6) In the vortex region in which the vorticity is lower than the background one, a process of energy dissipation into heat occurs.

It is assumed that the vortex destruction in the second phase may also be described within the framework of 2-D RANS if an appreciably higher background turbulence level and essentially lower scale are to be specified. The background turbulence in the phase concerned is not immediately related to that of the atmosphere but is generated by the vortex itself (secondary vorticity). With this, its key parameters will be the vortex circulation and wingspan. The idea has been implemented in the circulation loss computational program based on 2-D RANS using an algebraic turbulence model. Thus, the second phase may be described by the same equations but with different turbulent energy dissipation rate value ε_t, for in this phase the turbulent background is generated by the vortex filament itself due to the shortwave perturbation buildup. With this, the key quantities determining ε_t are the vortex circulation at the initial moment of time Γ_o and the distance between vortices b:

$$\varepsilon_t = C_3(1/b)(\Gamma_0/b)^3$$

For constant C_3, the value 0.0003 has been obtained. All empirical constants were obtained by means of its fitting to the results of some test cases published in [2] (lidar measurements).

As the time instant for ε_t changeover (the moment of phase transition), an empirical criterion is used:

$$T^* = \min(T_{\text{link}}, 8t_o)$$

where T_{link} is the vortex contact time according to the linear theory [15].

E. New Theoretical Vortex Diffusion Model

A new theoretical model of the vortex destruction in a turbulent atmosphere is suggested that substantiates every item of the semi-empirical model described earlier. Wake vortices are characterized by the fact that in the vortex region the vorticity longitudinal component is much greater than the lateral one $|\omega_x| \gg \sqrt{|\omega_y|^2 + |\omega_z|^2}$. Yet, on the vortex periphery the longitudinal component decreases exponentially and is comparable on the order of magnitude with the turbulent atmosphere background vorticity. It should be emphasized that the turbulent atmosphere vortices are essentially three dimensional and that the wake vortices are two dimensional, at least until they begin to link or become deformed by turbulence; in other words, inside the wake vortex the two-dimensional approach is valid and 2-D RANS may be used.

It should be noted that the atmosphere turbulence scale is much greater than the vortex diameter and distance between vortices b. In compliance with Kolmogorov's theory for the uniform and isotropic turbulence, the atmosphere turbulent energy is distributed over the vortex cascade from the atmosphere turbulence scale size to the viscosity scale. Thus, an appreciable fraction of the atmosphere turbulent energy falls into the same scale as the order of the vortex size.

It is obvious that on the vortex periphery the two-dimensional approach becomes invalid. With this, there occurs a strong interaction between the two-dimensional wake vortices and the three-dimensional vortices of the turbulent atmosphere on the same scale as the order of the vortex size; hence, the two-dimensional wake vortices are transformed into three-dimensional vortices of the turbulent background. Because of the vortex diffusion, increasingly larger vortex areas are transferred into the turbulent background, which accounts for the vortex circulation "loss." This mechanism is valid for the first (slow) phase of the vortex turbulent diffusion and characterized by appreciable pulsations as the vortex circulation decreases, which is observed in the experiment. It is for this reason that the definition of the vortex circulation as an average value over the ring $r = 5$–15 m (the vortex diameter is on the order of 10 m) has been empirically introduced.

After a while, as the wake vortex grows weaker, the vorticity inside the vortex itself begins to strongly interact with the background one, that is, there comes the second phase of the vortex destruction. The phase is characterized by strong velocity fluctuations in the entire vortex region that cause circulation exchange between positive and negative vortices. This results in fast wake destruction.

On the results of the analysis carried out, the following conclusions can be drawn:

1) The circulation loss effect is a result of the vortex interaction on its periphery with the three-dimensional vortices of the background vorticity on the same scale as the order of the vortex size.

2) The circulation loss effect may be described by 2-D RANS using only semi-empirical turbulence models that evidently allow for the turbulent energy influx from the large-scale atmosphere turbulent vortices into the wake vortex region.

An alternative to item 2 may be the usage of 3-D RANS with a modified turbulence model to allow for the streamline curvature.

F. Sinusoidal Instability

The experiments show that two parallel vortices gradually begin to perform symmetric oscillations with increasing amplitude. Over the course of time, the vortex plaits combine to form a ring system, after

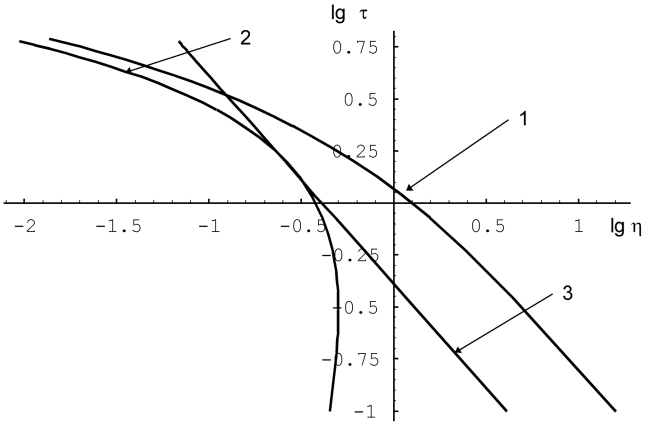

Fig. 7 Vortex life span, where 1 denotes [16], 2 denotes weak turbulence [15] $\eta = 0.87\tau^{1/4}e^{-0.83\tau}$, and 3 denotes strong turbulence [15] $\eta = 0.41/\tau$.

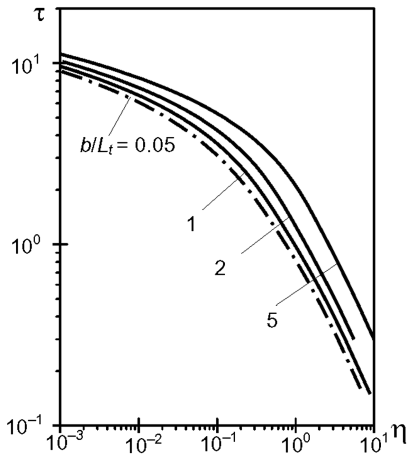

Fig. 8 Effect of parameter b/L_t on the dimensionless vortex life span.

which the vortex wake is quickly destructed. Crow [11] succeeded in simplifying the evolution problem of a vortex wake consisting of two vortices with circulation of different signs. By introducing certain simplifications, a system of equations has been obtained that describe a change in the shape of the plaits in space. To characterize the turbulence intensity, a dimensionless parameter $\eta = \varepsilon^{1/3}2\pi b^{4/3}/\Gamma$ is used, which is related to the Karman model parameters through the following ratio:

$$\eta = \sqrt{\frac{1}{a}\frac{55}{9\pi\alpha_k^{5/3}}}\bar{\sigma}\left(\frac{b}{L}\right)^{1/3} \approx 1.09\frac{\bar{\sigma}}{a^{1/2}}\left(\frac{b}{L}\right)^{1/3}$$

where $\bar{\sigma} = \sigma 2\pi b/\Gamma$, and $a \approx 1.5$ is the Kolmogorov's constant [see Eq. (5)]. It is suggested that the characteristic evolution time T_{link} of the unstable oscillations be calculated based on condition $\sigma_{\Delta y_S} = b$. The nondimensional vortex life span may be introduced by the formula $\tau = T_{\text{link}}/(2\pi b^2/\Gamma)$.

In [11], a continuous spectrum of eigenvalues for the problem concerned is analyzed and those with maximum real part (complex numbers) are found. A comparison with the experimental data showed that the estimates obtained correctly assessed, both qualitatively and quantitatively, the nature of the vortex wake evolution. The phenomenon described (increasing vortex plait symmetric oscillations with definite frequency) was called the "Crow sinusoidal instability."

Table 2 Time of the vortex ring formation

q, m/s	0.1	1.0
T_{link} [15], s	170	48
T_{link} (modified) [18], s	212	66
T_{link} (Karman linear theory) [21], s	162	62
T_{delay}, s ($L_2 = 20$ m)	229	41

The atmospheric turbulence is a major external perturbation stimulating the onset of oscillations. Crow and Bate [15] considered linearized equations of the vortex perturbed motion under the effect of turbulence described by the Kolmogorov model. In the time instant T, when the symmetric oscillation rms becomes equal to the initial distance between vortices $\sigma_{\Delta y_S} = b_0$, the vortices are believed to come in contact, break up, and recontact with subsequent ring formation, which results in fast vortex wake destruction. Thus, the wake life span is determined.

Because the atmosphere turbulence is a random process, time instant T (the wake life span) is also a random quantity. In [15], the formulas determining the average wake life span T are obtained for the weak and strong turbulence separately. Dynnikov [16] solved the problem in the same statement, but without division into cases of weak and strong turbulence, and presented a complete solution that, in particular, renders the results in [15] for the case of the strong turbulence more precise (Fig. 7).

In the analysis of the case considered in [15], the distance between vortices b was taken as a turbulence scale. This choice of turbulence scale results in a detraction of the relative turbulence level at the same turbulence dissipation rate ε. Dynnikov's results [16] allow the wake average life span values for the case of strong turbulence to be specified (the wake average life span increases a bit) and confirm the estimates in [15] for the most interesting case of weak turbulence.

According to Crow [11], oscillations of a pair of vortices about an unperturbed position are divided into symmetric and antisymmetric mode shapes that are determined relative to their functions:

$$\Delta y_S(x,t) = \Delta y_2(x,t) - \Delta y_1(x,t)$$
$$\Delta z_S(x,t) = \Delta z_1(x,t) + \Delta z_2(x,t)$$

for the symmetric shape and

$$\Delta y_S(x,t) = \Delta y_1(x,t) + \Delta y_2(x,t)$$
$$\Delta z_S(x,t) = \Delta z_2(x,t) - \Delta z_1(x,t)$$

for the antisymmetric one. Here, variables Δy_1, Δy_2, Δz_1, and Δz_2 designate displacements in the vortex plane (lateral displacement) and perpendicular to the plane (vertical displacement) for the first and second vortex, respectively.

Differential equations for the Fourier transformation on variable x for the lateral and vertical components of the symmetric mode are [11,17]

$$\frac{\partial \Delta\hat{y}_S}{\partial t} = a_{12}\Delta\hat{z}_S + (\hat{v}_2 - \hat{v}_1), \qquad \frac{\partial \Delta\hat{z}_S}{\partial t} = a_{21}\Delta\hat{y}_S + (\hat{w}_2 - \hat{w}_1)$$

Coefficients a_{12} and a_{21} for the symmetric mode are described by relations [17]

$$a_{12}(\beta) = (\Gamma/2\pi b^2)[1 - \psi(\beta) + \beta^2\omega(\delta)],$$
$$a_{21}(\beta) = (\Gamma/2\pi b^2)[1 + \chi(\beta) - \beta^2\omega(\delta)]$$

where $\beta = kb, \delta = \beta\frac{d}{b}$, $\omega(\delta) = \frac{1}{2}\left[\frac{(\cos\delta - 1)}{\delta^2} + \frac{\sin\delta}{\delta} - Ci(\delta)\right]$, $\chi(\beta) = \beta K_1(\beta)$, $\psi(\beta) = \beta^2 K_0(\beta) + \beta K_1(\beta)$, $K_0(\beta)$ and $K_1(\beta)$ are the modified Bessel functions, and d is the vortex plait diameter. For the case of the antisymmetric mode, the equations for the Fourier transformation for the lateral and vertical oscillation components are of the following form:

$$\frac{\partial \Delta\hat{y}_A}{\tau t} = a_{12}\Delta\hat{z}_A + (\hat{v}_2 - \hat{v}_1), \qquad \frac{\partial \Delta\hat{z}_A}{\partial t} = a_{21}\Delta\hat{y}_A + (\hat{w}_2 - \hat{w}_1)$$

where $a_{12}(\beta) = (\Gamma/2\pi b^2)[1 + \psi(\beta) + \beta^2\omega(\delta)]$, $a_{21}(\beta) = (\Gamma/2\pi b^2)[1 - \chi(\beta) - \beta^2\omega(\delta)]$.

The vertical and lateral wind gust sum and difference spectral densities for the Karman model are [18]

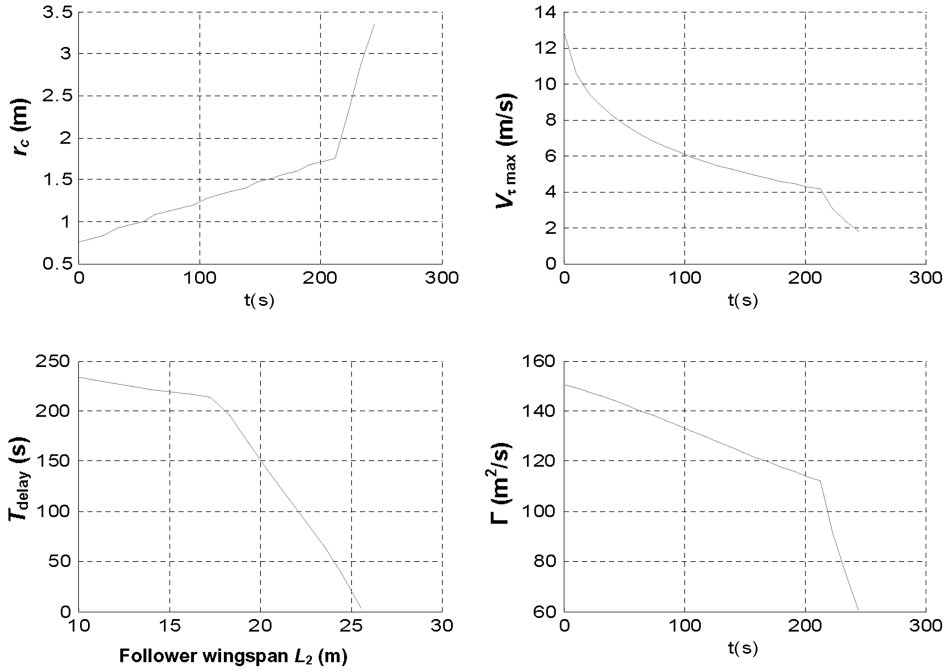

Fig. 9 Vortex parameters and safe time interval at $q = 0.1$ m/s (Tu-204).

$$S_{v_1 \pm v_2}(\beta) = \frac{4\sigma_v^2}{\pi\alpha_k}\left(\frac{b}{\alpha L_v}\right)^{\frac{2}{3}} \frac{1}{\beta_v^{5/3}}\left\{\left[\frac{1}{2} \pm \left(\frac{\beta_v}{2}\right)^{\frac{5}{6}} \frac{K_{5/6}(\beta_v)}{\Gamma(5/6)}\right] + \frac{5}{3}\left(\frac{\beta}{\beta_v}\right)^2\left[\frac{1}{2} \pm \left(\frac{\beta_v}{2}\right)^{\frac{11}{6}} \frac{K_{11/6}(\beta_v)}{\Gamma(11/6)}\right]\right\}$$

$$S_{w_1 \pm w_2}(\beta) = \frac{32\sigma_w^2}{3\pi\alpha_k}\left(\frac{b}{\alpha_k L_w}\right)^{\frac{2}{3}} \frac{1}{\beta_w^{5/3}}\left\{\left[\frac{1}{2} \pm \left(\frac{\beta_w}{2}\right)^{\frac{5}{6}} \frac{K_{5/6}(\beta_w)}{\Gamma(5/6)}\right] - \frac{5}{8}\left(\frac{b}{\alpha_k L_w \beta_w}\right)^2\left[\frac{1}{2} \pm \left(\frac{\beta_w}{2}\right)^{\frac{11}{6}} \frac{K_{11/6}(\beta_w)}{\Gamma(11/6)}\right]\right\}$$

where $\beta_v^2 = (kb)^2 + (b/\alpha_k L_v)^2$ and $\beta_w^2 = (kb)^2 + (b/\alpha_k L_w)^2$. In studying the effect of turbulence on the evolution of unstable vortex oscillations, the Kolmogorov model [11] with the spectral density energy function is used:

$$E(\Omega) = a\varepsilon^{2/3}/\Omega^{5/3} \tag{5}$$

The Kolmogorov model advantage is that it contains one parameter instead of two. Justification for the model application usually lies in the fact that the ratio of distance between vortices b to

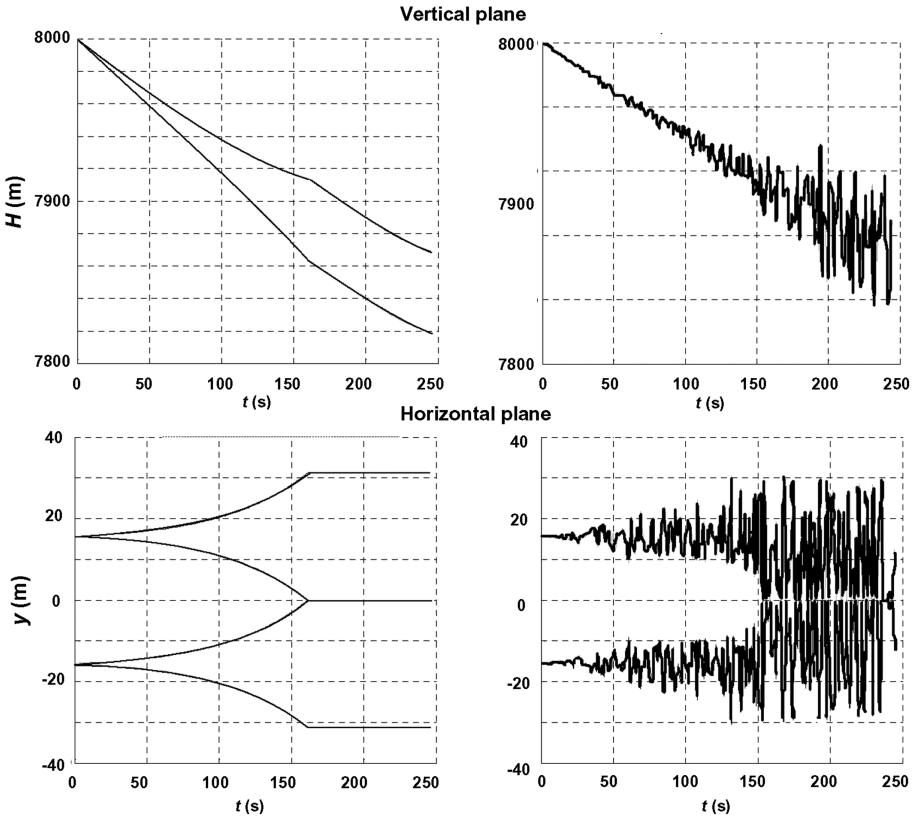

Fig. 10 Zones of possible wake location in the vertical and horizontal planes at $q = 0.1$ m/s (the risk corridor is on the left, whereas one of the wake vortex path realizations is on the right).

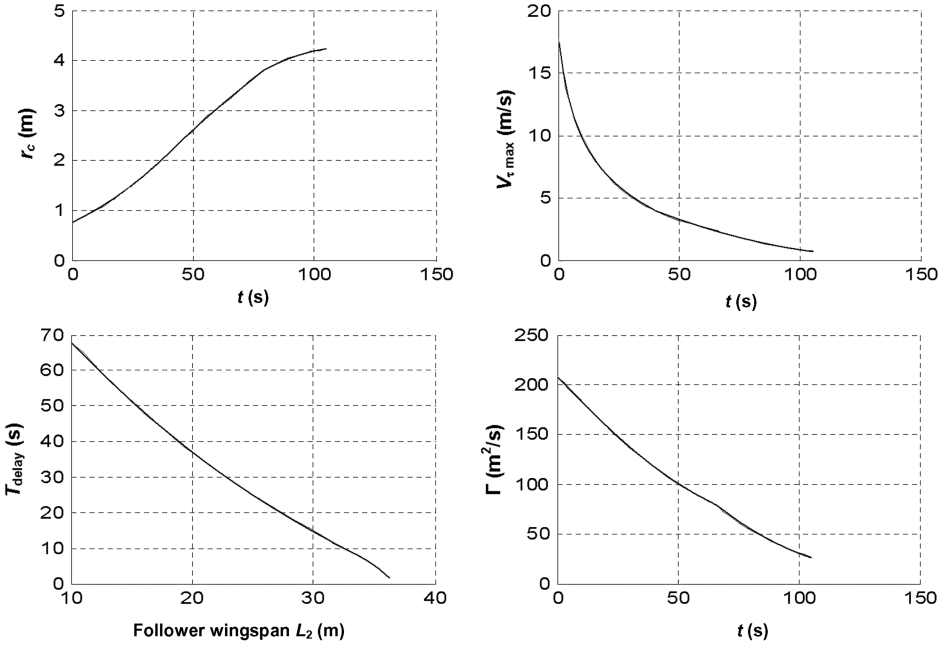

Fig. 11 Vortex parameters at $q = 1$ m/s.

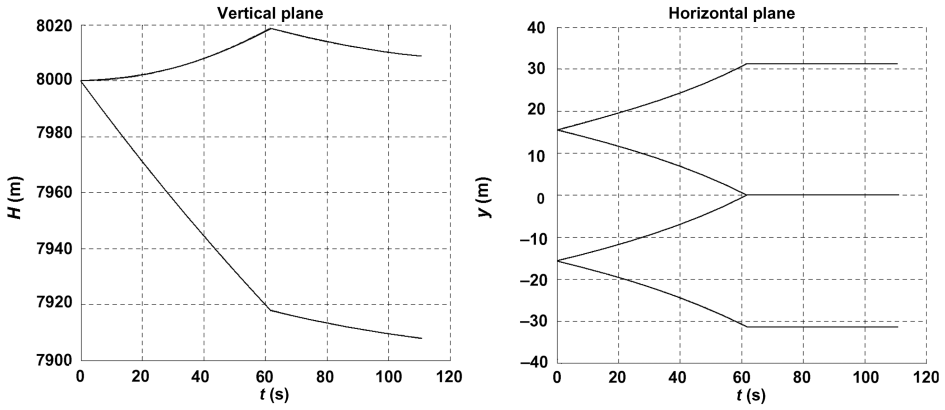

Fig. 12 Zones of possible wake location at $q = 1$ m/s.

the turbulence scale L_t is small, and in this case only high frequencies affect the evolution of unstable oscillations. By comparing Eqs. (2) and (5) at high-frequency values, it is easy to establish the relationship between parameters of the two models:

$$a\varepsilon^{2/3} = \frac{55}{9\pi}\frac{1}{\alpha_k^{5/3}L_t^{2/3}}\sigma^2$$

Figure 8 presents the effect of parameter b/L_t on the dimensionless vortex "life span." It follows from the results presented that the universal relationship $\tau(\eta)$ [11] for the Kolmogorov model ($b/L_t = 0$) is sufficiently accurate for important, practical cases except for the low-flight altitudes at which relation b/L_t may be high.

The average wake life span is a highly significant parameter for evaluating the threat level for the aircraft following the wake generator. It might be noted in connection with this that, when in the landing stage, substituting the elliptical circulation distribution (optimal in the sense of induced drag minimization) by that close to the triangular one (realized by the aircraft inboard flap deflections) may result in significant decrease in the time specified owing to the distance between vortices b diminishing. Hence, a substitution like that may appear to be advantageous.

The following figures offer an illustration of the calculations for the Tu-204 layout; Table 2 presents calculated values for the time of the vortex ring formation using the classical Crow–Bate theory (the Kolmogorov spectrum [11]) and its modification [18], as well as calculation results based on the present paper technique (the Karman spectrum) for turbulence levels $q = 0.1$ and 1 m/s.

Figure 9 gives detailed wake characteristics (time dependence of the core radius, circumferential speed maximum, and vortex circulation, as well as the follower safe delay interval as a function of its wing span L_2). Figure 10 presents vortex paths (risk corridors) and an illustration of a stochastic trajectory that fills in the risk corridor as well. Here and in what follows the risk corridor size has been determined based on the vortex path coordinate scatter criterion σ. The same data for the turbulence level $q = 1$ m/s are given in Figs. 11 and 12.

It follows from the data presented that aircraft flight inside the risk corridor is prohibitive due to a high probability of encountering the preceding aircraft's wake vortex. The risk corridor size is determined by the stochastic properties of the wake vortex paths rather than by the vortex core size, which is much less than that of the risk corridor. The second aircraft safe time interval is not related to the vortex ring formation time and may be both greater and less than the latter.

V. Application of the Wake Mathematical Models for Flight Safety Problem Solutions

In terms of the wake model, every airport is characterized by the wind statistics in variables V–q (wind velocity–turbulence level). The airport characteristics are obtained with the aid of the standard record processing of the meteorological tower wind-gauge readings taken for several years (Fig. 13).

Based on the results obtained and using the Monin–Obukhov model, the L_{MO} value is determined for the lower and upper curves in the plane $V - q$. All the experimental points lie in the area between them. For a typical airport located on a plain (e.g., Frankfurt Airport), practically all the atmosphere states occupy the area between the curves $L_{MO} = -1$ and 10 m. Analysis of the circulation attenuation shows that the most hazardous are steady modes (the lowest turbulence level at a specified wind velocity).

The key verification of the wake model suggested is the correct estimation of the safe distance (safe time interval) between the aircraft when landing on the same landing strip. As an example, a safe interval aft of different aircraft were calculated. The atmosphere parameters were taken on the curve $L_{MO} = 10$ m. Table 3 presents the estimates obtained for the safe time interval, and the ICAO regulations as well. It should be noted that the atmosphere parameters at $L_{MO} = 10$ m and $V = 2$ m/s are the worst in terms of the flight safety. At such a lateral wind velocity, the windward vortex of the wake from preceding aircraft will stay under the runway and will have the minimum dissipation rate.

In the 1970s in the United States (NASA/Federal Aviation Administration), a program of flight tests was conducted to determine the safe distance between aircraft pairs. Figure 14 presents a summary table of the test results. A significant scatter is seen to exist in evaluating the safe distances for a particular aircraft pair relative to the atmosphere state. Figure 15 gives the vortex attenuation calculation results compared to the data of the lidar maximum velocity measurements in the vortex aft of B747 under the Frankfurt Airport conditions with different atmosphere states.

Figure 16 gives calculation results of the leeward vortex position aft of B747 against measurement data [19]. Figure 17 shows safe time intervals for aircraft with wingspans L when landing on the same landing strip aft of the aircraft indicated. Chosen is the worst of the cases with $q = 0.2$ m/s, $L_{MO} = 10$ m, and $V_{10} = 2$ m/s (wind velocity at $H = 10$ m).

The ICAO regulations are also plotted here (a heavy class refers to aircraft with $L > 40$ m, a middle one with -20 m $< L < 40$ m, and a light one with $-L < 20$ m). The aircraft A380-200 is not seen to meet the ICAO regulations, which requires that a new class be introduced to the safe separation matrix. Flight experiments conducted by Airbus have completely substantiated the conclusion drawn and are also presented in Fig. 17 (see footnote ¶). It should be noted that, according to the ICAO recommendations, the delay time is constant in every class and based on the worst case.

Table 3 Time delay

Follower	Time interval (calculation), s		ICAO regulations, s
	$V = 5$ m/s	$V = 2$ m/s	
B747	40	65	106
A340	50	100	106
A310	70	110	106
A320	100	135	132
Learjet	130	165	159

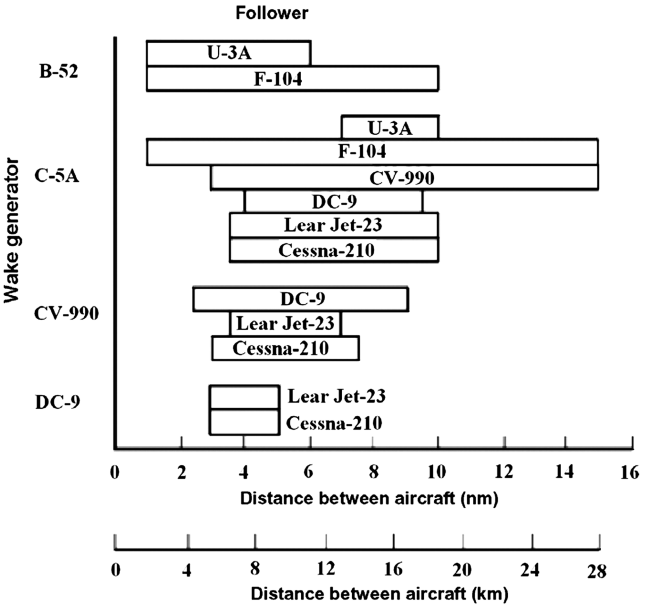

Fig. 14 Safe distance estimation based on test results vs aircraft types and atmosphere state [20].

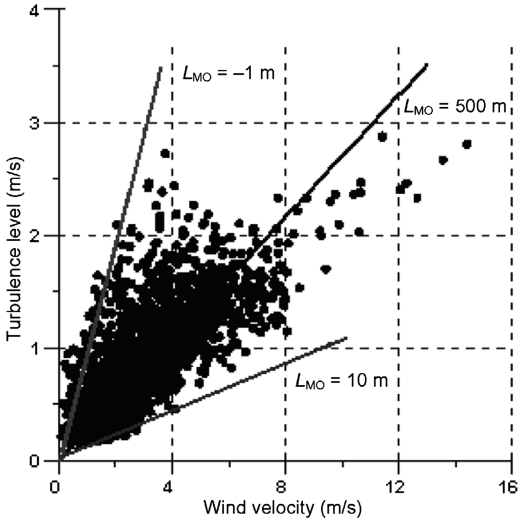

Fig. 13 The ICAO model complies with the neutral wind $|L_{MO}| > 400$. The area within the lines $L_{MO} = -1$ and 10 m is the range of the wind velocity and turbulence level values predicted by the Monin—Obukhov model.

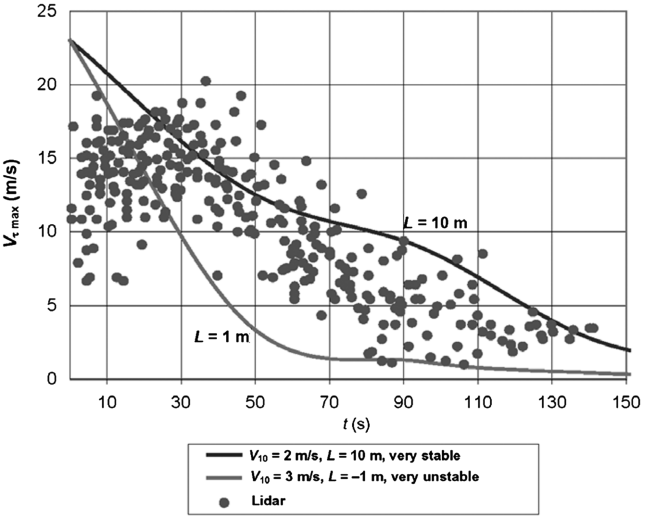

Fig. 15 Maximum vortex velocity aft of B747 (2-D RANS calculation, lidar [19]).

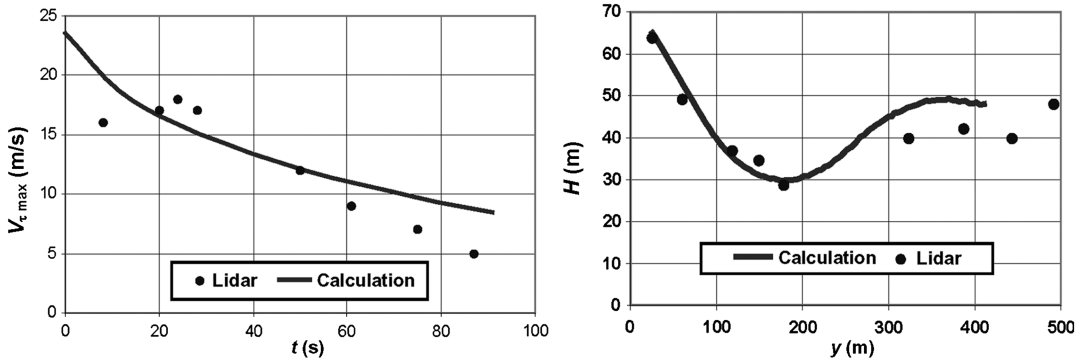

Fig. 16 Leeward vortex evolution aft of B747 (2-D RANS calculation, lidar [19]): a) maximum velocity in the vortex, and b) vortex path. (Stable atmosphere $L_{MO} = 20$ m and wind velocity $V = 4.6$ m/s at $H = 65$ m).

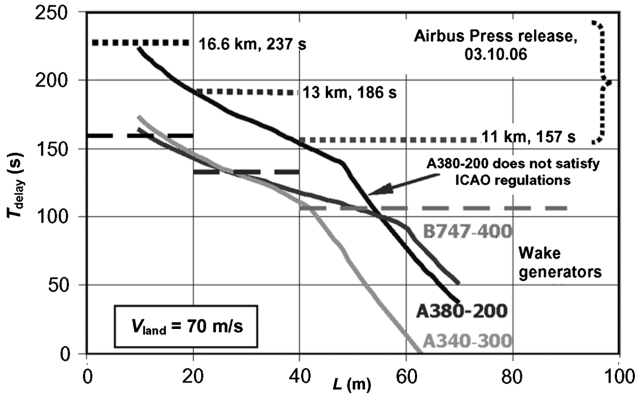

Fig. 17 Safe time intervals for aircraft with wingspans L when landing on the same landing strip aft of the aircraft indicated.

VI. Conclusions

On the results of the theoretical analysis carried out in the present paper, the following conclusions can be drawn. The effect of circulation loss is the result of the wake vortex periphery interaction with the three-dimensional vortices of background vorticity of the scale as the order of the wake vortex size. This cannot be described by a two-dimensional approximation without introducing empirical models of the vortex circulation attenuation. Both phases of the vortex destruction may be specified using the boundary-value problem for 3-D RANS with a modified turbulence model. The method of 3-D LES should be used only for modeling a small-scale instability, which is essential at takeoff and landing, in low-altitude flights, and in the presence of atmosphere temperature stratification only.

The following conclusions can be drawn from the results of the calculations performed in the paper. An aircraft flight within the risk corridor is prohibitive due to a high probability of encountering the wake vortex generated by the preceding aircraft. The risk corridor is not a measure of our lack of knowledge of the potential vortex path but is an actual danger caused by the chaotic behavior of the latter. A special emphasis should be laid on the fact that the risk corridor size is determined by the wake trajectory stochastic properties rather than by the vortex core radius, for which the size is much less than that of the risk corridor. The safe distance is not related to the time of the growth of the sinusoidal instability up to the moment when the vortices come into contact (with the subsequent vortex rings formation). It may be both higher and lower than T_{link}.

Acknowledgments

The work has been performed with support from the Russian Basic Research Fund, grant no. 07-08-13582, as well as the Analytical Departmental Task Program (no. 2.1.1/200) of "the development of the higher school scientific potential (2009–2010)." The authors would especially like to thank G. S. Byuschgens (Russian Academy of Science), who lent his support for the present work. We are also grateful to V. P. Kuzmin, without whom the research concerned would not be complete, and I. S. Bosnyakov, who has performed a set of numerical calculations. We also want to express our deep gratitude to Jens Konopka, Deutsche Flugsicherung, GmbH, who granted statistical data on the atmospheric conditions of the Frankfurt Airport to us. Some stages of the investigations have been discussed with Philippe Spalart, the Boeing Company; Klaus Huenecke, Daimler–Benz Aerospace Airbus; and Vernon Rossow, NASA.

References

[1] Gerz, T., Holzäpfel, F., and Darracq, D., "Commercial Aircraft Wake Vortices," *Progress in Aerospace Sciences*, No. 3, 2002, pp. 181–208. doi:10.1016/S0376-0421(02)00004-0

[2] Shen, S., Ding, F., Han, J., Lin, Y.-L., Arya, S. P., and Proctor, F. H., "Numerical Modeling Studies of Wake Vortices: Real Case Simulation," AIAA Paper 0755, 1999.

[3] Belotserkovsky, S. M., Dvorak, A. V., Zhelannikov, A. I., and Kotovsky, V. N., "Computer Simulation of Turbulent Jets and Wakes," *Problems of Turbulent Flows*, Izdatel'stvo Nauka, Moscow, 1987, pp. 129–134.

[4] Vyshinsky, V. V., Zamyatin, A. N., and Soudakov, G. G., "Theoretical and Experimental Study of the Vortex Wake Evolution Behind the Aircraft Flying in the Atmosphere Boundary Layer," *Tekhnika Vozdushnogo Flota*, Nos. 3–4, 2006, pp. 25–38.

[5] Vyshinsky, V. V., and Soudakov, G. G., "Mathematical Model of the Vortex Wake Evolution Behind the Aircraft in the Turbulent Atmosphere," *Aeromechanika i Gasovaya Dynamika*, No. 3, 2003, pp. 46–55.

[6] Vyshinsky, V. V., and Soudakov, G. G., *The Aircraft Vortex Wake in the Turbulent Atmosphere (Physical and Mathematical Models)*, Trudy TsAGI, Moscow, 2005, pp. 1–156.

[7] Voyevodin, A. V., and Soudakov, G. G., "Flow over combination wing-body with flow separation from the wing lateral edges," *Uchenye zapiski TSAGI*, Vol. 19, No. 1, 1988, pp. 98–101 (in Russian).

[8] Shur, M. L., Strelets, M. K., Travin, A. K., and Spalar, P. R., "Turbulence Modeling in Rotating and Curved Channels: Assessing the Spalart–Shur correction," *AIAA Journal*, Vol. 38, No. 5, 2000, pp. 784–792. doi:10.2514/2.1058

[9] Etkin, B., *Dynamics of Atmospheric Flight*, Wiley, New York, 1972, pp. 1–580.

[10] Landau, L. D., and Lifschits, E. M., *Theoretical physics*, Vol. 6, Hydrodynamics, Izdatel'stvo Nauka, Moscow, 1988, pp. 1–736.

[11] Crow, S. C., "Stability Theory for a Pair of Trailing Vortices in a Turbulent Atmosphere," *AIAA Journal*, Vol. 8, No. 12, 1970, pp. 2172–2179. doi:10.2514/3.6083

[12] Kuzmin, V. P., and Yaroshevsky, V. A., *Estimation of the Dynamic System Phase Coordinate Limiting Deviations in Case of Random Disturbances*, Izdatel'stvo Nauka, Moscow, 1995, pp. 1–304.

[13] Saffman, P. G., "Structure of Turbulent Line Vortices," *Physics of Fluids*, Vol. 16, No. 8, 1973, pp. 1181–1188. doi:10.1063/1.1694496

[14] Rubinstein, R., and Zhou, Ye., "The Dissipation Rate Transport Equation and Subgrid-Scale Models in Rotating Turbulence," Institute

for Computer Applications in Science and Engineering Rept. 97-63, 1997; also NASA CR-97-206250.

[15] Crow, S. C., and Bate, E. R., "Lifespan of Trailing Vortices in a Turbulent Atmosphere," *Journal of Aircraft*, Vol. 13, No. 7, 1976, pp. 476–482.
doi:10.2514/3.44537

[16] Dynnikov, A. A., "Development of the Vortex Wake Instability Under The Turbulent Atmosphere Effect," *Investigation of Vortex Wake Evolution and Flight Safety Problems*, Vol. 2622, Trudy TsAGI, Moscow, 1996, pp. 119–128.

[17] Charney, J. J., Kaplan, M. L., Lin, Y.-L., and Pfeiffer, K. D., "A New Eddy Dissipation Rate Formulation for the Terminal Area PBL Prediction System (TAPPS)," AIAA Paper 2000-624, 2000.

[18] Kuzmin, V. P., "Estimation of Wake-Vortex Separation Distances for Approaching Aircraft," *Investigation of Vortex Wake Evolution and Flight Safety Problems*, Vol. 2627, Trudy TsAGI, Moscow, 1997, pp. 209–224.

[19] Köpp, F., "Doppler Lidar Investigation of Wake Vortex Transport Between Closely Spaced Parallel Runways," *AIAA Journal*, Vol. 32, No. 4, 1994, pp. 805–810.
doi:10.2514/3.12057

[20] Rossow, V., "Lift-Generated Vortex Wakes of Subsonic Transport Aircraft," *Progress in Aerospace Sciences*, Vol. 35, No. 6, 1999, pp. 507–660.
doi:10.1016/S0376-0421(99)00006-8

[21] Sarpkaya, T., "New Model for Vortex Decay in the Atmosphere," *Journal of Aircraft*, Vol. 37, No. 1, 2000, pp. 53–61.
doi:10.2514/2.2561